SMC-TR-94-48

AEROSPACE REPORT NO.
TR-94(4478)-3

Development of Welded Solar Arrays for DMSP and GPS Satellites

15 September 1994

Prepared by

P. C. BRENNAN
Mechanics and Materials Technology Center
Technology Operations

Prepared for

SPACE AND MISSILE SYSTEMS CENTER
AIR FORCE MATERIEL COMMAND
2430 E. El Segundo Boulevard
Los Angeles Air Force Base, CA 90245

Contract No. F04701-93-C-0094

Programs Group

THE AEROSPACE CORPORATION
El Segundo, California

This report was submitted by The Aerospace Corporation, El Segundo, CA 90245-4691, under Contract No. F04701-93-C-0094 with the Space and Missile Systems Center, 2430 E. El Segundo Blvd., Los Angeles Air Force Base, CA 90245. It was reviewed and approved for The Aerospace Corporation by S. Feuerstein, Principal Director, Mechanics and Materials Technology Center. Lt. Col. S. L. Woida and Capt. Jim Luke were the project officers for the program.

This report has been reviewed by the Public Affairs Office (PAS) and is releasable to the National Technical Information Service (NTIS). At NTIS, it will be available to the general public, including foreign nationals.

This technical report has been reviewed and is approved for publication. Publication of this report does not constitute Air Force approval of the report's findings or conclusions. It is published only for the exchange and stimulation of ideas.

S. L. Woida, Lt. Col. USAF
SMC/CIE

FOR

Jim Luke, Capt. USAF
SMC/CZS

REPORT DOCUMENTATION PAGE

Form Approved
OMB No. 0704-0188

1. AGENCY USE ONLY (*Leave blank*)	2. REPORT DATE	3. REPORT TYPE AND DATES COVERED
	15 September 1994	

4. TITLE AND SUBTITLE

Development of Welded Solar Arrays for DMSP and GPS Satellites

5. FUNDING NUMBERS

F04701-93-C-0094

6. AUTHOR(S)

Brennan, P. C.

7. PERFORMING ORGANIZATION NAME(S) AND ADDRESS(ES)

The Aerospace Corporation
Technology Operations
El Segundo, CA 90245-4691

8. PERFORMING ORGANIZATION REPORT NUMBER

TR-94(4478)-3

9. SPONSORING/MONITORING AGENCY NAME(S) AND ADDRESS(ES)

Space and Missile Systems Center
Air Force Materiel Command
2430 E. El Segundo Boulevard
Los Angeles Air Force Base, CA 90245

10. SPONSORING/MONITORING AGENCY REPORT NUMBER

SMC-TR-94-48

11. SUPPLEMENTARY NOTES

12a. DISTRIBUTION/AVAILABILITY STATEMENT

Approved for public release; distribution unlimited

12b. DISTRIBUTION CODE

13. ABSTRACT (*Maximum 200 words*)

The integrity of welds used to join solar cells to interconnect materials was investigated in two development programs, one for DMSP and the second for GPS. Previous solar arrays for these programs utilized soldering to join the interconnect to the cells. It is critical to both programs to demonstrate the ability of the welded interconnects to withstand the thermal cycling expected on orbit. Initial test boards for DMSP indicated that additional development was necessary to generate a weld process capable of meeting mission requirements. The Aerospace Corporation was successful in improving the weld survival rates for DMSP, but ultimately recommended that the process be abandoned in favor of an alternate weld design or solder approach. The GPS design was much more successful. Weld evaluations before and after thermal cycling indicated that the GPS design was capable of surpassing mission requirements. An SEM evaluation technique, mechanical fatigue tester, and a rapid thermal-cycle tester were designed in support of these programs. This report relates the findings generated during the two development programs and discusses the reasons behind the failure of the DMSP weld program and the success of the GPS program.

14. SUBJECT TERMS	15. NUMBER OF PAGES
Solar arrays, Welding, Silver, Thermal cycles, DMSP, GPS, Fatigue	33
	16. PRICE CODE

17. SECURITY CLASSIFICATION OF REPORT	18. SECURITY CLASSIFICATION OF THIS PAGE	19. SECURITY CLASSIFICATION OF ABSTRACT	20. LIMITATION OF ABSTRACT
UNCLASSIFIED	UNCLASSIFIED	UNCLASSIFIED	

Preface

The author would like to acknowledge the assistance of R. Brose, A. Garcia, C. Hoover, R. A. Jamieson, J. Marcus, B. Nelson, E. Pierre-Louis, F. Ross, and J. Wasynczuk for their assistance during this investigation.

The author also acknowledges the assistance of Martin Marietta Corporation in technical discussions and for providing the solar cell assemblies.

Contents

Figures

1. Introduction

Development of welding techniques to attach silicon (Si) solar cells to metallic cell interconnects was the subject of two long-term programs undertaken by Martin Marietta (MM) Astro Space Division (E. Windsor, NJ and Valley Forge, PA) for the Defense Metereological Satellite Program (DMSP) and Global Positioning Satellite (GPS) Program. The welded interconnects, which were designed to replace soldered joints, were necessary to improve long-term interconnect integrity and high-temperature performance. The Aerospace Corporation was involved in the development programs since their inception; however, the Mechanics and Materials Technology Center (MMTC) was not approached to investigate the integrity of the welded interconnects until late in the DMSP development program (March 1993). At that time, an intense investigation of weld integrity was undertaken by MMTC.[1-3,6] Our investigation was prompted by poor survivability after thermal cycling of the resistance welds between the vapor-deposited silver (Ag) layer on DMSP solar cells and the Ag mesh that serves to interconnect adjacent solar cells. Chronologically, the GPS study followed the DMSP investigation. Aerospace played a key role in GPS weld development from the program inception.[4,5]

The DMSP welded interconnect was designed and developed by MM. MM subcontracted with Applied Solar Energy Corp. (ASEC) (City of Industry, CA) to develop a welded interconnect for GPS capable of withstanding the stresses generated during on-orbit thermal cycling. The two programs used different approaches in their attempts to satisfy mission requirements. These differences will be discussed in this report.

No hardware with welded interconnects has yet flown for either program. Previous solar arrays produced by MM utilized soldered interconnects. Because the solar arrays operate at high homologous temperatures (temperature/absolute melting temperature) during sun exposure on orbit, the microstructure of the solder will undergo changes and coarsen with time. The cyclic temperature range for testing DMSP cells is –80 to +80°C. The cyclic temperature range for testing GPS cells is –146 to +71°C. In both cases, the on-orbit temperature range is slightly less severe by a few degrees. Every cycle between hot and cold results in the array components expanding and contracting according to their individual coefficients of thermal expansion (CTE). Large thermal stresses build up and act on the solder joints because of the differences in thermal expansion behavior. These stresses, acting under cyclic conditions, can strain the joints to failure under a low cycle fatigue (LCF) type mode. CTEs vary with temperature, but over the temperature range of interest, the CTE for Invar is approximately 1×10^{-6}/°C. The CTE for Si is approximately 3×10^{-6}/°C, whereas the CTE for Ag is 19×10^{-6}/°C. The vapor-deposited Ag layer on the Si cell, since it is only 6μm thick, expands and contracts in approximately the same manner as the base Si, which is much thicker [approx. 0.010" (250 μm)]. Hence, stresses build up and promote failure at the joint between the cell and interconnect. Separation of welds diminishes the solar array's capability to supply the necessary power for the satellite to operate properly.

Schematics of DMSP and GPS cells are shown in Figure 1. The DMSP interconnect is made from an all-Ag mesh. Initially, 0.0020" (50.8 μm) thick mesh was used for the interconnect. However, a switch was made to 0.0010" (25.4 μm) thick mesh. The reason for this change will be discussed

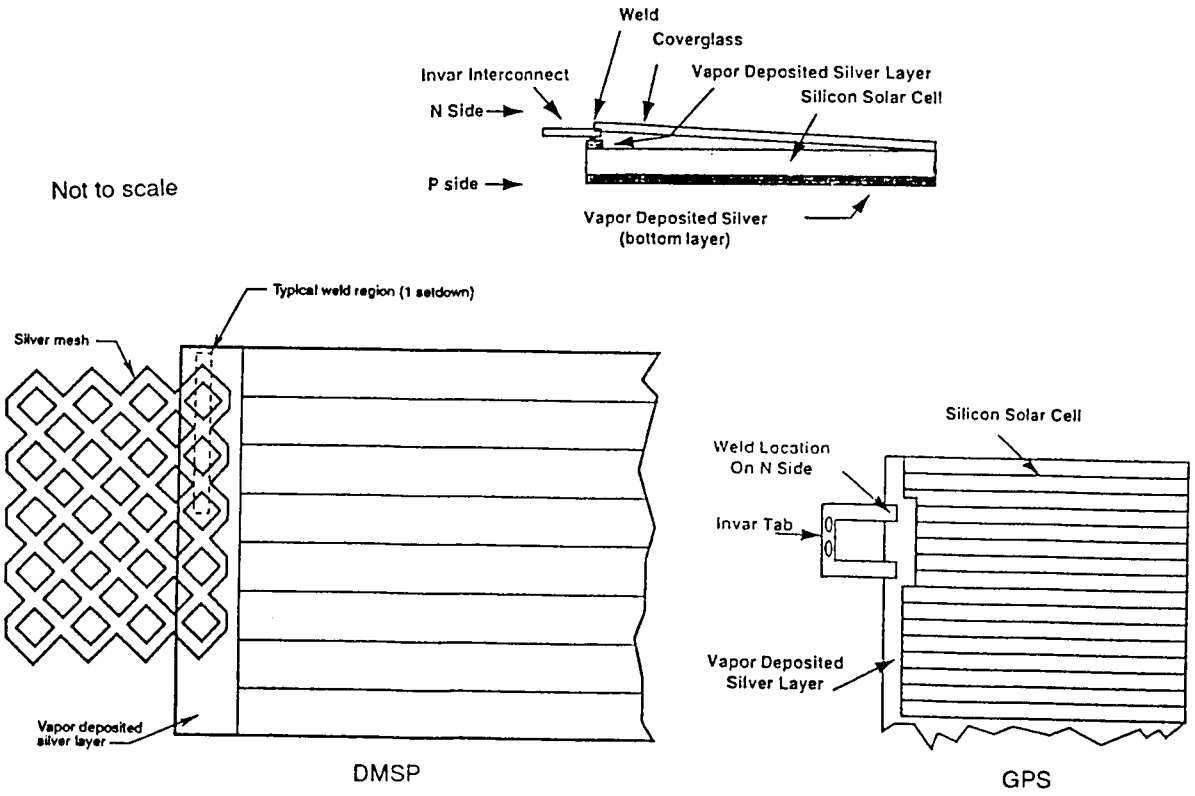

Figure 1. Schematics of DMSP and GPS solar cell/interconnect assemblies.

later. The mesh is fabricated in one of two ways: the expanded mesh technique (0.0020") or the chemical etching technique (0.0010"). In the expanded mesh technique, slits are first introduced into a Ag sheet. The sheet is then stretched, and the slits expand into diamond-shaped openings. The chemical etching technique utilizes a non-reactive mask to remove Ag in select areas and produce the appropriate pattern. The two techniques have a strong effect on the weld quality, which will also be discussed later. The GPS interconnect consists of an Invar core [0.0010 ±0.0001", (25.4 μm)] with a Ni strike, Cu plating [0.00005–0.00015", (1.3–3.8 μm)] and Ag plating [0.0002–0.0004", (5.1–10.2 μm)] on both exposed faces. The composition of Invar is 64% Fe, 36% Ni. To facilitate bonding between the interconnect and the solar cell, a 0.236" (6 μm) thick Ag layer is vapor deposited on the Si DMSP and GPS solar cells. The GPS interconnect design is different from the interconnect used on earlier GPS satellites, which used all-Ag interconnects like the DMSP cells. The GPS Invar interconnect was studied for use in place of an all-Ag interconnect because its CTE more closely approximates that of Si, reducing the propensity for thermal fatigue at the bond interface.

It was critical to the development programs to demonstrate the ability of the welded interconnects to withstand the thermal cycling expected on orbit. The life requirement for DMSP satellites is approximately 15,000 cycles between –80 and +80°C. The life requirement for GPS cells is 1860 cycles between –146 and +71°C. To demonstrate the integrity of the design, the contractor must

demonstrate that the array can function after a period twice as long as the intended on-orbit life. This translates to a requirement of 31,000 thermal cycles between –80 and +80°C for DMSP cells and 3720 thermal cycles between –146 and +71°C for GPS cells.

A physical probing technique was employed by MM to map the surviving DMSP welds after thermal cycling. This technique involved wiggling the mesh with tweezers to determine if it was still adherent to the Si cell. Since this technique could damage welds and give false positive or false negative indications, a technique involving the scanning electron microscope (SEM) was eventually adopted for use. The goal of the SEM evaluation was to determine the number and location of weld sites still connecting the solar cells to the interconnects after thermal cycle testing and to determine the manner in which the welds failed, either during thermal cycling or during the destructive physical analysis. The SEM technique allowed for quick observation and classification of the fracture surfaces and weld quality. The SEM technique was also extremely useful in evaluating process changes. This SEM technique is described in detail later in this report.

Because thermal cycling of DMSP solar cells from –80 to +80°C in the MM facility required approximately three months to complete 31,000 cycles, accelerated testing involving larger temperature ranges and fewer thermal cycles was often used. In order to properly relate the accelerated and non-accelerated thermal tests, it is necessary to fully understand the stress conditions operating on the solar cell, especially at the interconnect joint. Cycling between –170 and +70°C (MM, E. Windsor, NJ), and –120 and +120°C (NASA-Lewis, OH) for 4000 and 5000 cycles, respectively, were thought to approximate the on-orbit thermal experience for DMSP. The GPS program, because of the far fewer thermal cycles, did not utilize accelerated testing. Accelerated testing would still take several weeks to complete. A faster means of evaluating process changes and alternative designs was sought. Two techniques were developed by MMTC. In the first, a mechanical fatigue tester was adapted to test interconnect joints at loads of less than one pound. This technique permitted thousands of cycles to be completed in a matter of minutes. In the second approach, a thermal cycling machine was set up to cycle solar cells between a liquid nitrogen (LN_2) bath (–196°C) and a steam chamber (approx. 85°C). This apparatus was capable of cycling cells at a much faster rate than the apparatus used by MM. These techniques are described in detail in this report.

Only strong welds can survive the severe on-orbit thermal cycling experienced by the solar cells. Weak and medium-strength welds may quickly fail due to thermal fatigue. For this reason, development of strong, high-quality welds was imperative to the success of the programs. Both the original weld quality and the stress level experienced at the weld joint strongly affect fatigue life. Also, the joint design can strongly affect the weld survival rate. DMSP and GPS use drastically different interconnect designs. Numerous design changes were proposed and investigated by Aerospace for the DMSP interconnect. This report reviews our efforts to improve the weld process for both the DMSP and GPS solar-cell interconnects from a metallurgical viewpoint. Prior to the completion of this study, a decision was made to continue using soldering as the mesh joining method for DMSP solar arrays. In contrast, GPS has decided to use welding on future satellite solar arrays.

2.3 Mechanical Fatigue Testing

A Fatigue Dynamics Inc. fatigue precracker was used to mechanically fatigue the DMSP solar-cell interconnects. No mechanical fatigue testing was conducted on the GPS cells. Fixtures were made that allowed the cells to be clamped between Teflon sheets (Figure 2) in either a 0° or 90° configuration relative to the minor axis of the cell. The dimensions between the fixtures and amount of gripped material is given in Figure 3. A notch was machined into the fixtures to allow room for the stress-relief loop adjacent to the N bar. This loop relieves the stress between the cells connected in the series direction. The mesh was gripped in the upper fixture while the cell was gripped in the lower fixture. Since the 90° configuration most closely approximates the actual stress orientation, the majority of the tests were run in this configuration. The 90° orientation is shown in Figure 3. Because of the difference in thickness between the Ag mesh and the Si cell, it was necessary to use stainless-steel shims to properly align the upper and lower fixtures. Shims were also used in some tests to localize the gripping to the edge of the Ag mesh. The mesh is attached to the P side of the specimen along the approximate centerline of the cell. The N-side welds are on the N-bar, which is along the edge of the opposite side of the cell. The samples that were tested were all fabricated with expanded Ag mesh.

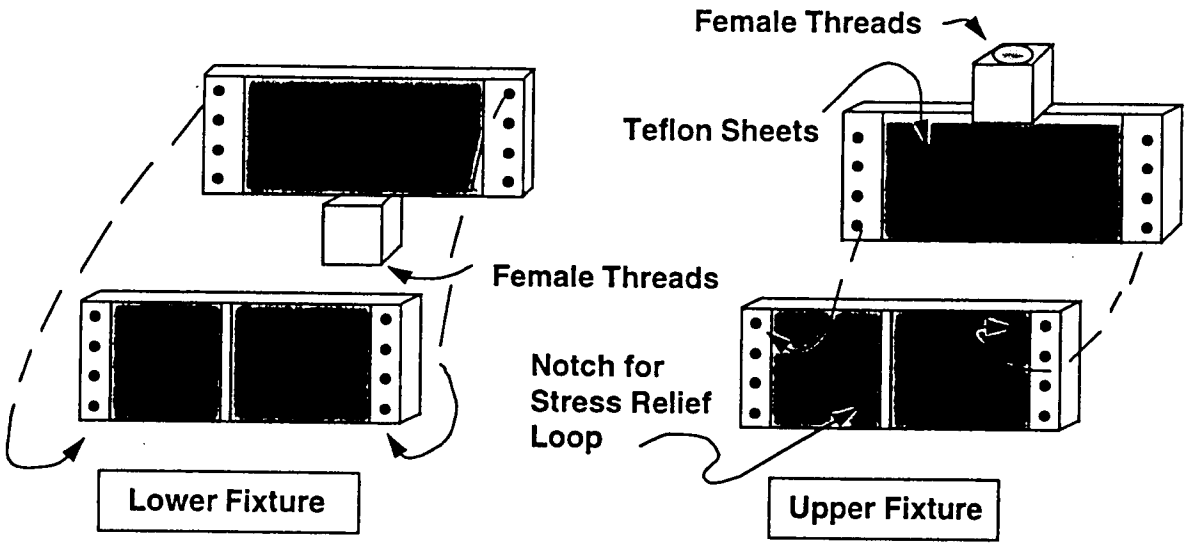

Figure 2. Schematics exhibiting design of mechanical fatigue testing fixtures.

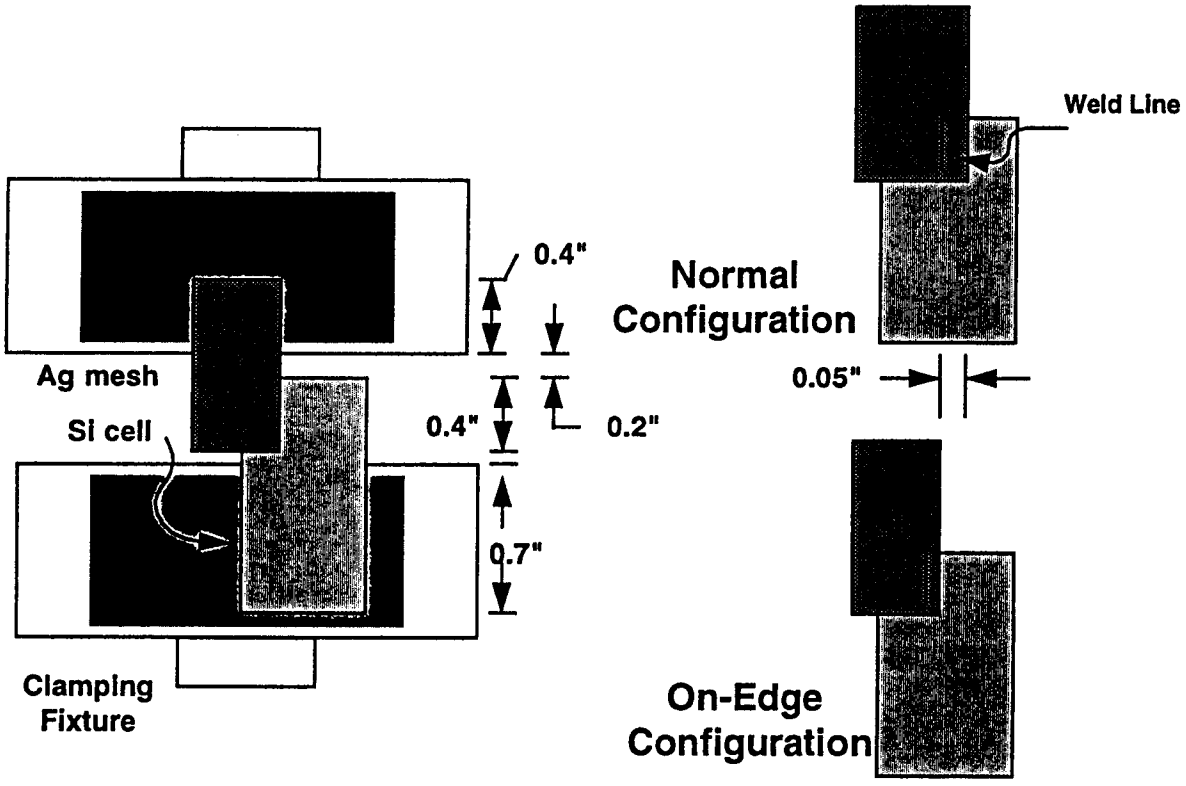

Figure 3. Schematics exhibiting typical sample set-up for mechanical fatigue testing.

A 100-lb load cell with an accuracy of 0.1% was used to measure the loads. A Fatigue Dynamics Inc. shutdown controller was used to control the number of test cycles. The data was recorded on an IBM XT computer via a Hewlett Packard rms voltmeter connected to the shutdown controller and a Strawberry Tree Inc. data acquisition card. The data were analyzed on Quattro Pro.

The fatigue precracker is a constant displacement machine. Each cycle displaces the lower fixture from the upper fixture by the same amount. This means that variations in cross-sectional area will translate into variations in the load-carrying capacity of the mesh. It was imperative then that the mesh be cut to the same dimensions for every test. The multiple Ag strands beneath each weld electrode allow for 3–4 welds each time the electrode sets down. In preparing the samples for testing, the mesh was cut so that only two setdowns were tested (6–8 welds). The quality of the mesh was critical in obtaining meaningful results. Because any imperfection along the border of the mesh could act as a stress concentrator, only samples with perfect borders were used. The mesh on certain P-side samples was cut so that the weld setdowns were immediately next to the edge of the mesh. After a test was complete, the mesh was peeled from the cell if it was still adherent. Fracture surfaces of representative samples were then evaluated on the SEM.

2.4 Thermal Fatigue Testing

A schematic of the thermal-cycle apparatus is shown in Figure 4. A steel-mesh cage was used to transport the solar cells between a LN_2 bath and a steam chamber. A variable-speed motor was used to lift the cage. The majority of the tests were conducted at a rotation rate of 3.5 min/rev. This allowed for a residence time in the steam of approximately 1 min. The residence time in the LN_2 depended on the liquid level, but was also approximately 1 min. Faster rates did not allow sufficient time to equilibrate the cage and sample temperature with the steam-chamber temperature. Consequently, after an extended period, ice would develop on the cage. By using a slower rotation rate, the samples and cage were resident in the steam chamber long enough to melt any ice and to equilibrate with the surroundings. Modifications to the weld location on the mesh and cell, as well as modifications to the mesh geometry were tested. A schematic of the various cell designs is exhibited in Figure 5.

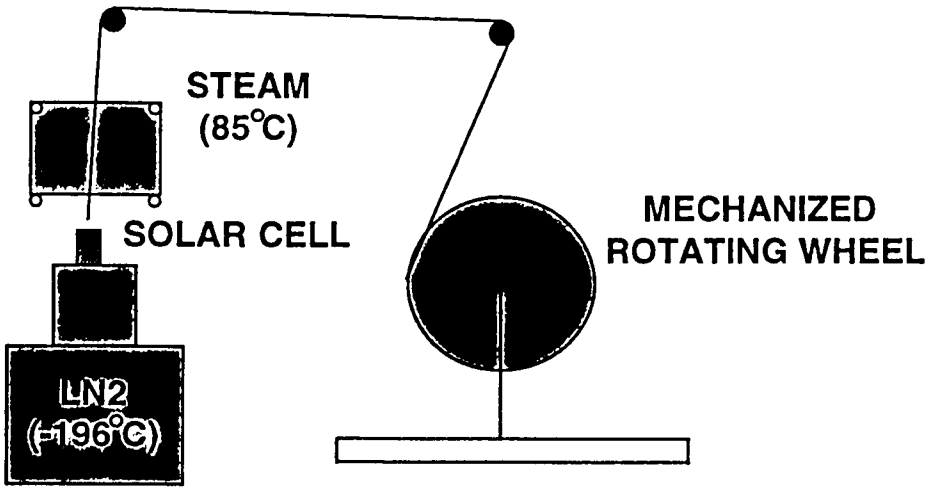

Figure 4. Schematic of solar cell thermal fatigue tester.

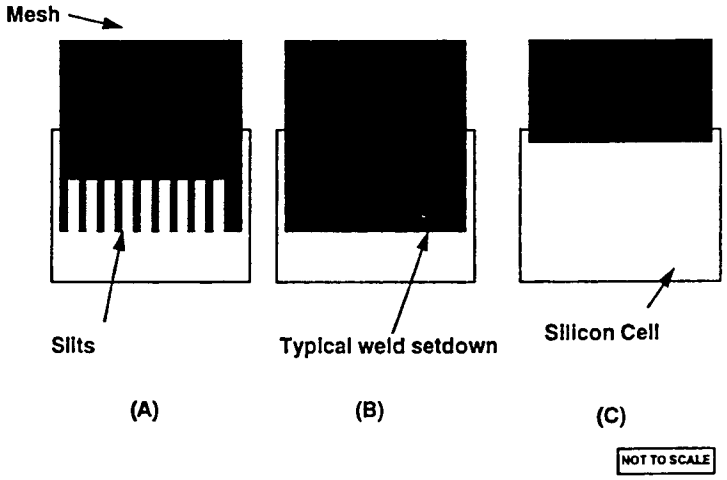

Figure 5. Schematic of basic cell designs tested in this study. (A) P-side sample with slits in mesh; (B) original P-side design with typical weld setdown location delineated; (C) basic design for all N-side welds and P-side edge samples designed to physically resemble N-side welds.

The apparatus and testing procedure were first qualified on Ag interconnects manufactured from expanded mesh. Later samples utilized etched-Ag mesh. The expanded mesh samples were fabricated with only eight setdowns per cell, in contrast to the etched mesh cells, which utilized ten setdowns per cell.

The temperature of the steam chamber was monitored with a type-K thermocouple. The temperature of the chamber would drop 10–15°C from its 85°C average when the chilled sample carrier first entered the chamber. The temperature would return to 85°C before the sample carrier exited the chamber. A temperature plot for an actual thermal cycle experienced by a 0.010"-diameter thermocouple is exhibited in Figure 6. The thermal experience for the solar cell should be similar. The test thermocouple was not calibrated. Consequently, there are errors in the absolute value of the indicated temperatures. Samples were allowed to cycle unattended for several-hour periods before requiring additional LN2 to be added to the bath.

Samples were investigated for evidence of weld failure on a daily basis. The location of adherent and failed regions was recorded after probing with tweezers. On the order of 100 cycles were typical between data points. After complete failure of the welds, the individual samples were removed from the sample carrier. Representative samples were then investigated on the SEM.

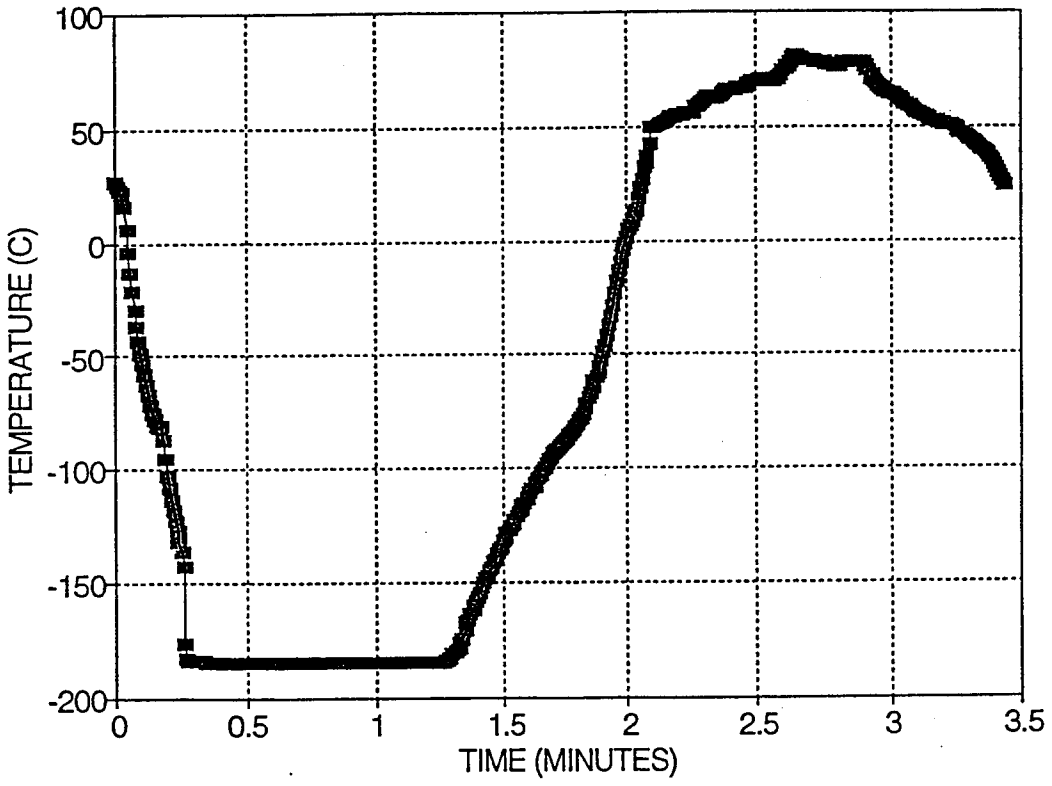

Figure 6. Temperature profile of a 0.010-in.-diam. type-K thermocouple as it cycles through one complete temperature cycle. Cycle time is approximately 3.5 min/rev. Notice uncalibrated thermocouple reads approximately 10°C off at liquid nitrogen temperature (–196°C).

3. Results and Discussion

3.1 DMSP

The DMSP weld development program preceded the GPS program. Consequently, much of the knowledge gained on the first program was utilized by the second. Multiple test boards were evaluated in MMTC and at MM (E. Windsor). Weld survival statistics were provided for each of the test boards. Initially, the survival rates for both the N- and P-side welds were not acceptable for mission requirements. When MMTC and other offices at Aerospace became involved, a concentrated effort was made to improve the weld survival rates. It should be noted that during the period MMTC was involved in this program, improvements were made which increased the N-side weld thermal-cycle survival rate dramatically from well below 50% to over 90%. Weld survival rates above 76% were desired. Similar dramatic improvements in the P-side survival rates were not seen. Some improvements were made in P-side weld survival but not to the extent of that experienced by the N side.

When a portion of a welded joint fails, the Ag mesh separates from the solar cell and leaves microstructural evidence of its failure mode. Adjacent areas that remain adherent are subject to the thermal stresses with each additional thermal cycle. Because of the adjacent adherent areas, the two failed surfaces come into contact with each other during every thermal cycle. This has the effect of mashing the two failed surfaces together. Sharp microstructural features become rounded, producing a crumbly appearance. Fewer thermal cycles have less opportunity to distort the fracture surface, and more ductile features are noted. In LCF (less than 100,000 cycles), a material fails by plastic strain as opposed to elastic strain, which is predominant for high-cycle fatigue. Plastic strains result in microvoid formation and the presence of dimples on fracture surfaces. Hence, the presence of ductile features is not contrary to that expected for a LCF fracture surface, and the presence of dimples alone is not a sufficient criterion for concluding that failure occurred by ductile overload fracture. Sharp tear ridges indicate that the failure occurred during removal of the mesh from the Si solar cell, as opposed to during thermal cycling. Conveniently, the desirable tear ridges appear brighter than other regions in the SEM. Both thermal fatigue and ductile-fracture-type failure modes are exhibited in Figure 7. The difference between the fracture modes is readily apparent to a trained eye.

Over the course of the weld development program, many factors were investigated that affected weld quality. One factor was the mesh fabrication technique. All of the soldered DMSP and GPS solar arrays previously manufactured used Ag mesh made from the expanded mesh technique. Expanded mesh is characterized by residual stresses from the initial forming operation and irregular surface features that inhibit uniform, consistent welding. During the DMSP development program, a switch was made to Ag mesh fabricated by means of chemical etching. This had an immediate positive effect on weld quality. The etched mesh is much smoother than the expanded mesh. Welds produced with etched mesh were more uniform and consistent; however, variations in weld survival rates remained.

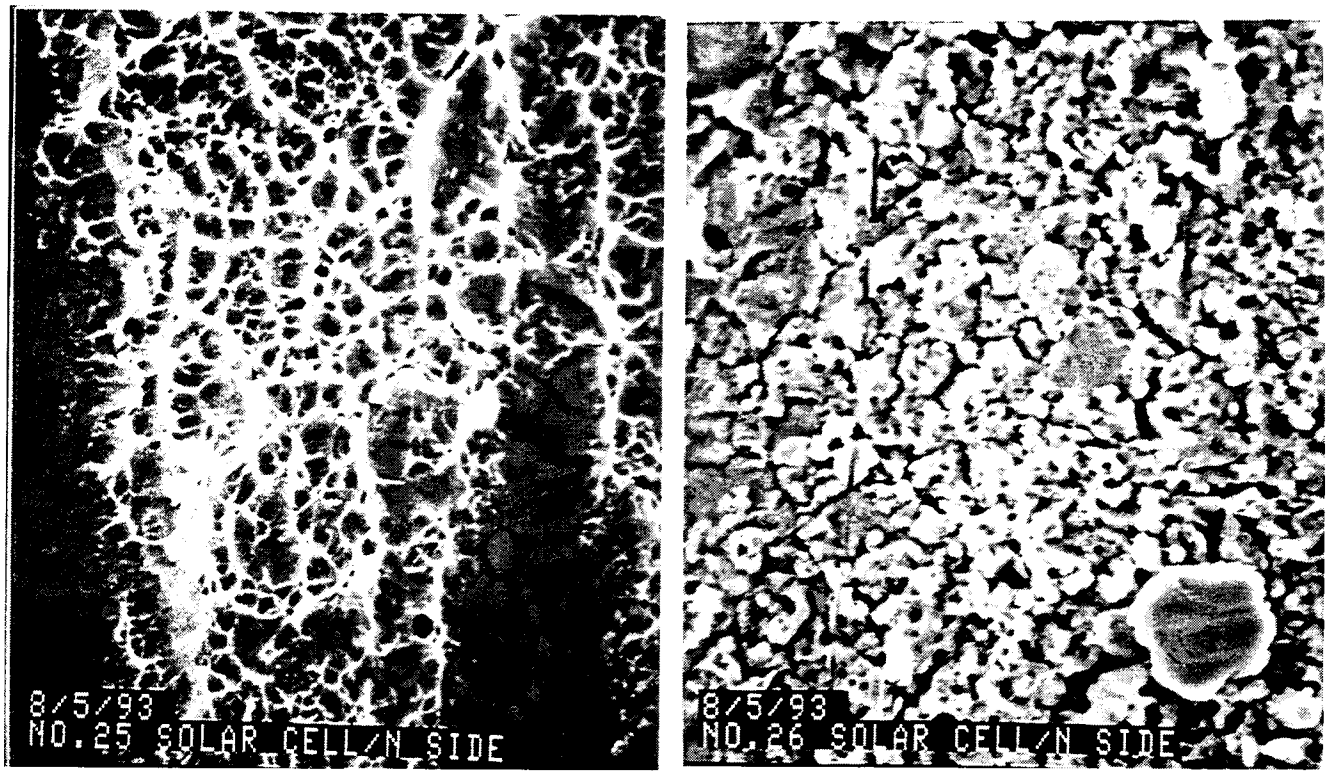

(a) (b)

Figure 7. Micrographs exhibiting differences between fracture modes. (a) dimpled rupture with sharp tear ridges, (b) thermal fatigue fracture with crumbly worked surface.

The surface roughness of the vapor-deposited surface can also account for weld variations. As exhibited in Figure 8, variations in height are evident between different Si grains, and between the edge and center of individual grains. The much smaller Ag grains are clearly delineated above the much larger Si grains. The Ag layer, since it is only 6μm thick, replicates the Si substrate morphology. Because of the inherent high and low regions on the interconnect and vapor-deposited layer, not all of a given area will weld to the cell. Without sufficient weld energy or electrode force, recessed regions will not weld with the opposing material, and an erratic weld pattern may form.

Equivalent parameter settings can result in varying weld qualities. Certain parameters, such as voltage, setdown pressure, surface temperature, and pre-weld circuit resistance, are monitored during the weld cycle. However, variations in these parameters may occur once the weld has begun to form, and the accuracy of the readings is not always clear. For instance, the apparent mesh surface temperature can be affected by the mesh surface reflectivity. The pre-weld circuit resistance is affected by the surface roughness, sulfide buildup, contact area, and setdown pressure, all of which can vary within allotted amounts. The pre-weld circuit resistance is a function of resistances at several locations. The resistance at the mesh/cell interface is of primary importance, but variations in resistance values at the electrode/mesh interface may interfere with any

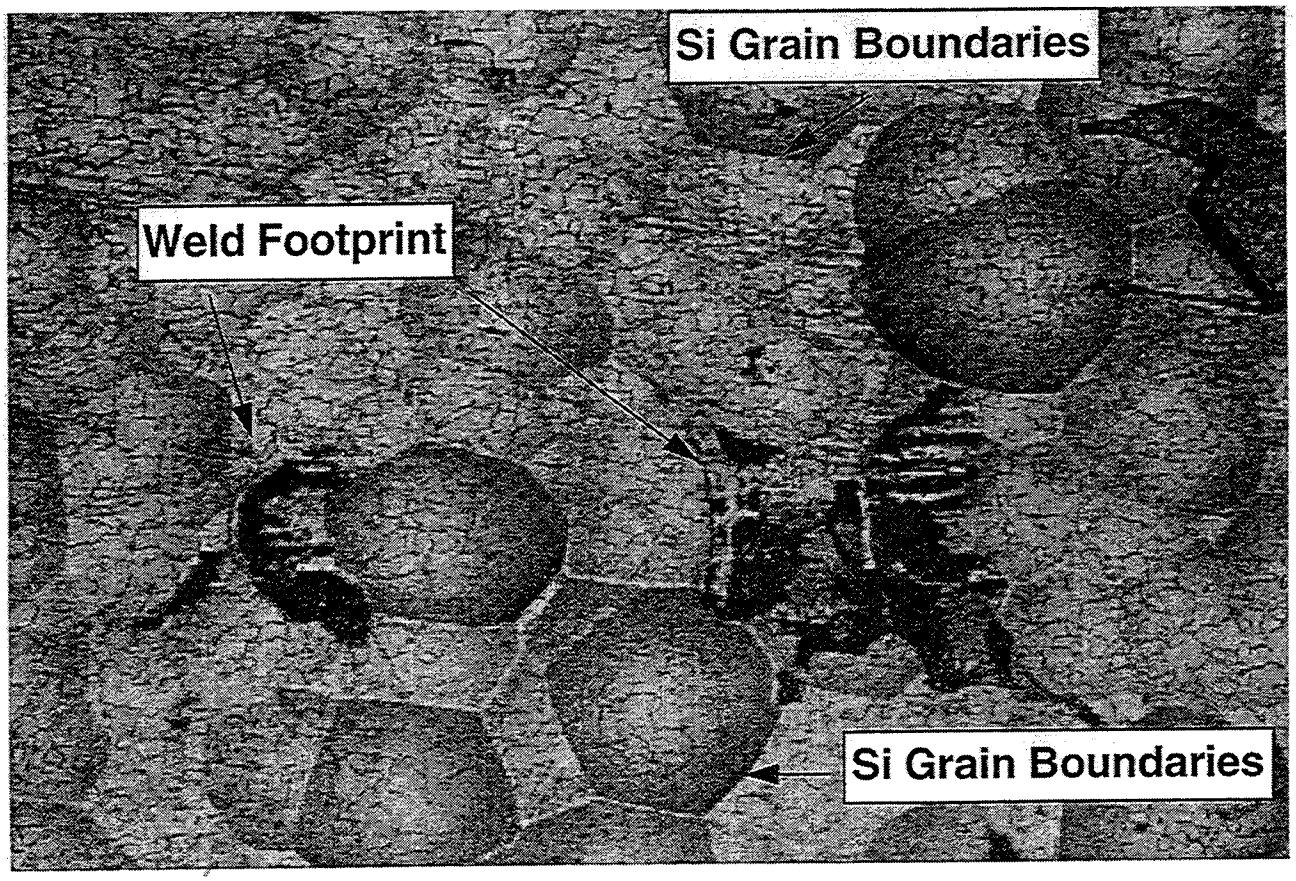

Figure 8. Optical micrograph exhibiting weld footprint, Si grain boundaries and non-uniformities in surface height.

attempt to accurately monitor this resistance. Resistance welding, by its very nature, is subject to variations, and weld-quality variations will always exist. Ideally, the weld parameters should be designed such that the poorest- and highest-quality welds expected from a given set of parameters will meet the mission requirements. With the parameters used for the DMSP etched mesh samples, the average N-side weld quality lay further above the border between success and failure than did the P-side welds. Few P-side welds were capable of surpassing the mission requirement, and many were significantly below mission requirements.

A typical, as-fabricated DMSP N-side weld is exhibited in Figure 9. Prior to being thermal cycled, the welds fail, of course, in a ductile manner. Sharp, bright tear ridges are readily visible at low magnifications in the SEM. After thermal cycling, the size of the indications decreases. A typical post-thermal-cycle, P-side setdown is shown at progressively higher magnifications in Figures 10a–c. At low magnification (Figure 10a), the indications appear as bright spots amongst the dull, non-welded Ag and thermally fatigued fracture regions. In Figure 10b, the distinction between regions is much clearer. At a much higher magnification (Figure 10c), the sharp tear ridges and well-defined dimples are readily visible. Organic "crud" from the RTV adhesive typically collects in wide regions on the P side of cells (see Figure 11). This material often made site location more difficult, but not impossible.

Figure 9. Typical as-fabricated DMSP N-side weld setdown.

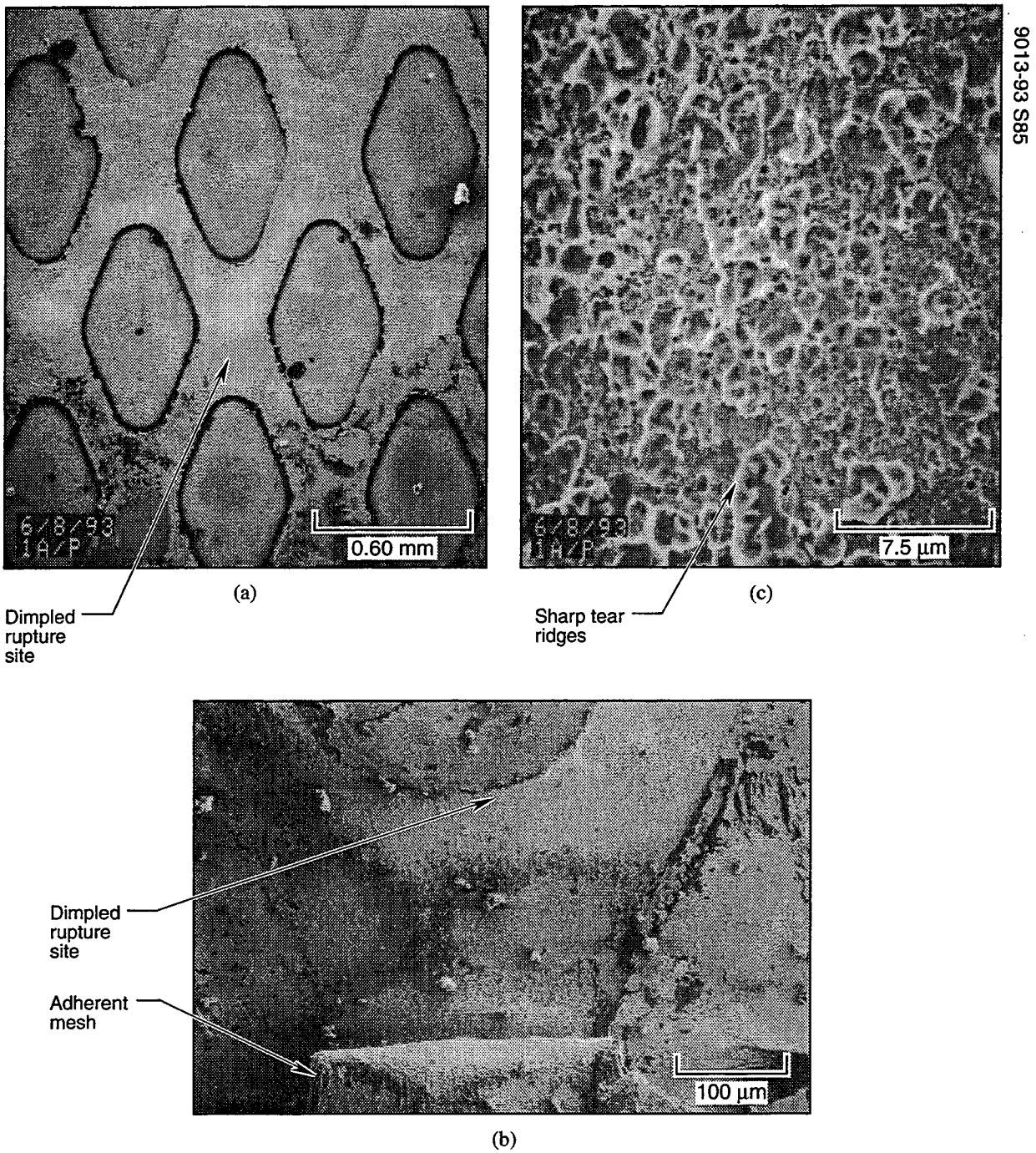

Figure 10. Micrographs exhibiting bright dimpled rupture regions at various magnifications for typical P-side welds.

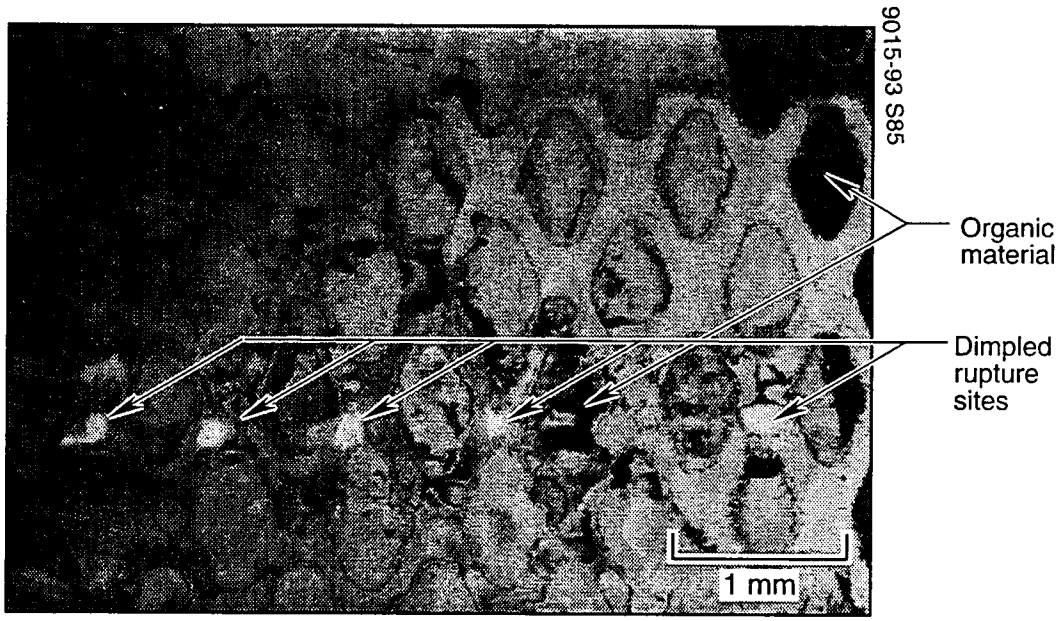

Figure 11. Micrograph exhibiting organic material that clouds the fracture surface regions making site identification on P-sides difficult.

Most notable was the disparate survival rates between N- and P-side welds. The number of successful N-side setdowns was typically greater than P-side setdowns. Typically two to three indications were found for each setdown. A typical post-thermal-cycle, N-side setdown is exhibited, at progressively higher magnifications, in Figure 12. Again, the ductile indications are readily apparent at low magnification. Pieces of adherent mesh were commonly seen while investigating the N side. In these cases, the mesh broke within the strands of the mesh while it was being peeled off the cell.

Metallographic cross sections were also used to investigate weld quality. As exhibited in Figure 13, there exists little to no grain growth across the weld interface. This bond, often described as a thermal-compression bond, does not involve diffusion between the two materials involved in the joint and is, thereby, weaker than a bond that involves melting and grain growth across the original interface.

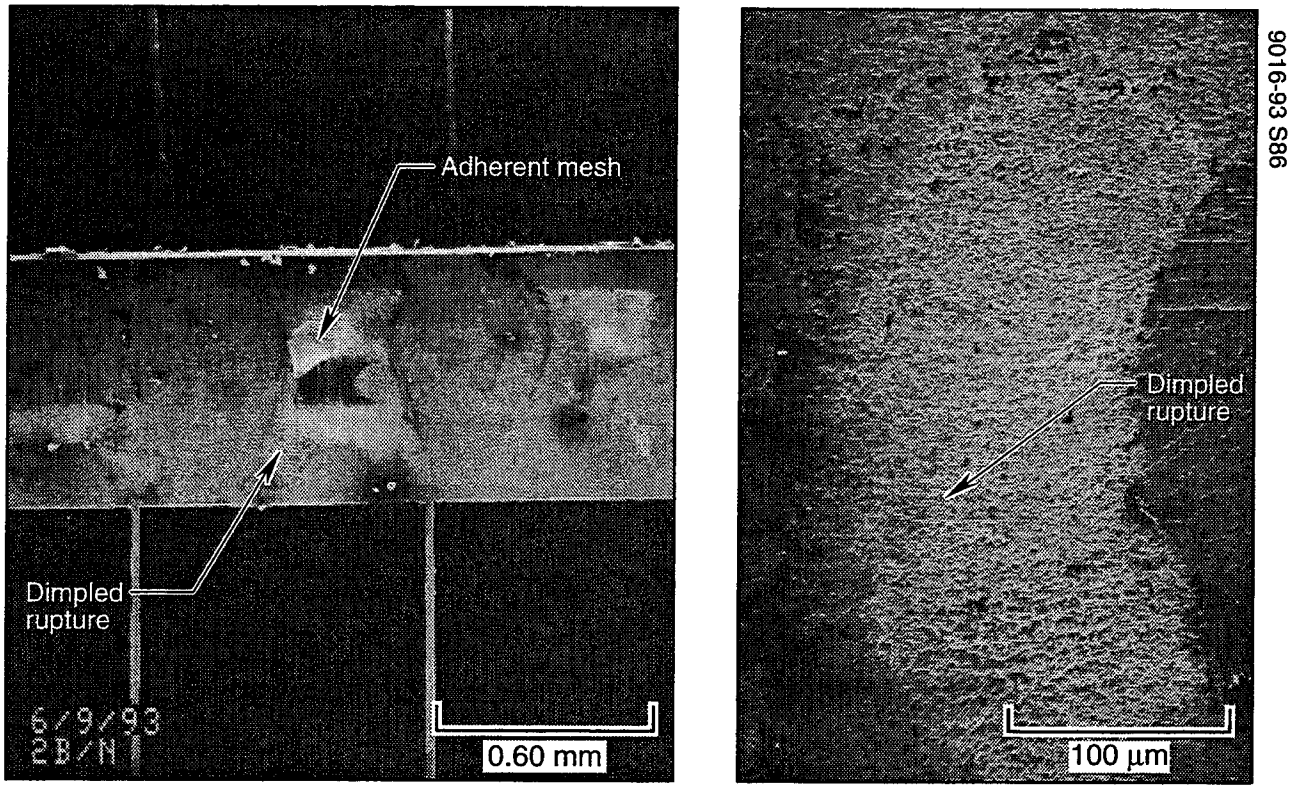

(a) (b)

Figure 12. Micrographs exhibiting bright dimpled rupture regions and adherent mesh for typical N-side welds.

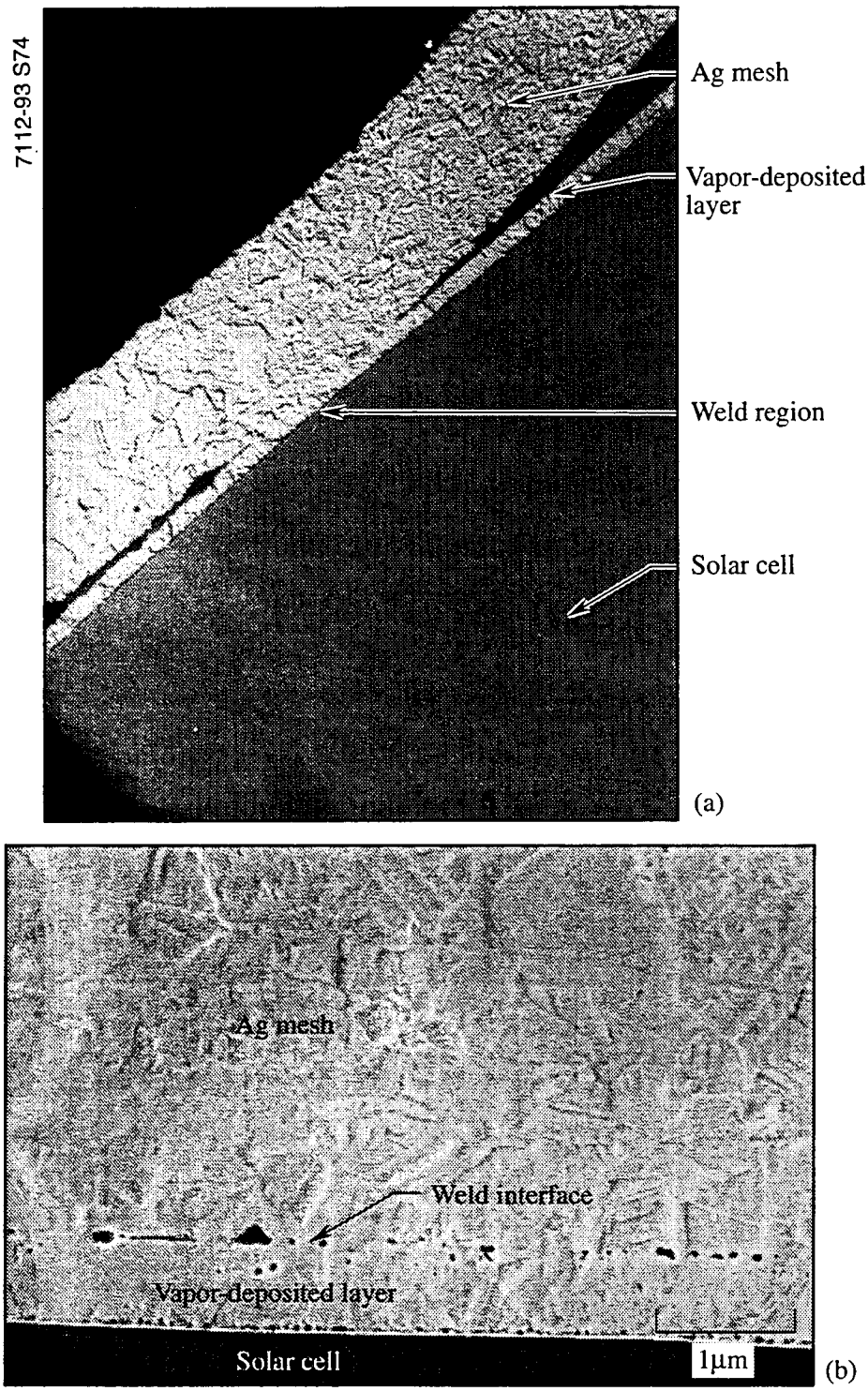

Figure 13. Cross-sectional view of photo-etched mesh adhered to the vapor-deposited layer. (a) low-magnification view; (b) higher-magnification view exhibits continuity of grain structure across weld interface.

The N-side indications were typically on the order of 50 × 50 μm^2. Many of the "best" indications were 100 × 100 μm^2 or larger. The corresponding non-thermal-cycled weld regions ranged from 250 × 200 μm^2 in the center of the mesh "X" to 250 × 125μm^2 in the individual mesh strands. Original weld areas varied because of scratches and variations along the mesh surface. Figure 14 exhibits the irregular shape of the original welds for a given setdown. No correlation between the indication size and the P or N side of the cell was noted.

The stress acting at the weld interface is higher for thicker mesh. Because of the problems with weld integrity after thermal cycling, an effort was made to reduce the stress acting on the weld interface by switching from 2-mil-thick Ag mesh to 1-mil-thick Ag mesh. The 1-mil N-side welds performed significantly better than the 2-mil N-side welds. The size, quantity, and distribution of ductile indications on the 1-mil N-side cells far surpassed those of the 2-mil N-side cells. This is due to stress reduction and improved weld formation with thinner mesh.

By the schedule-induced termination of the development program, the N-side survival rate appeared, on average, capable of meeting mission requirements. However, because of unexplained and unacceptable variations in N-side survival rates amongst cells and the less than

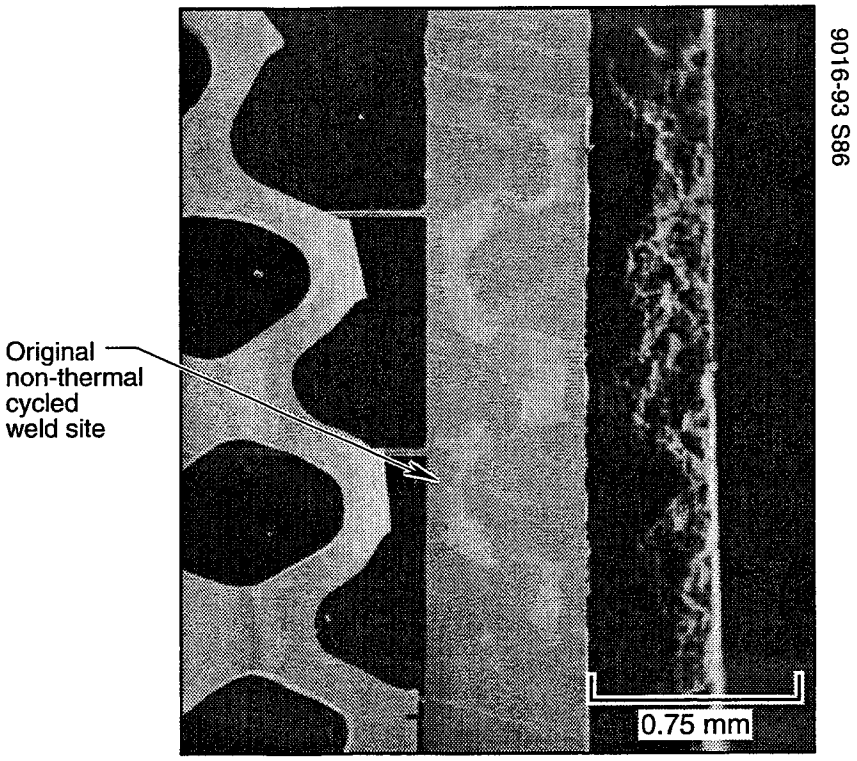

Figure 14. Micrograph exhibiting a typical irregularly shaped weld layout for a non-thermal-cycled solar cell.

acceptable P-side survival rates, the process was not approved. Significant improvements had been made in the welds. Still it was widely recognized that the high thermal conductivity and low electrical resistance of an all-Ag joint did not make for an optimum resistance-weld design. Interconnects made from materials such as Ag-plated Invar, Ag-plated Kovar, and Ag-plated molybdenum have been well known to the welded interconnect community for many years.[7] Insufficient time prevented acquisition and study of alternate materials for the DMSP solar arrays or a thorough investigation of alternate mesh geometries to lessen stresses acting at the weld interface. Because the GPS program was not as constrained by time as the DMSP, it was possible to study alternate materials and designs for the GPS program.

3.2 GPS

Representative fracture surfaces of GPS P-side welds are exhibited in Figure 15. The bond between the cell and the tab that was pulled off was very strong, and the bond failed below the

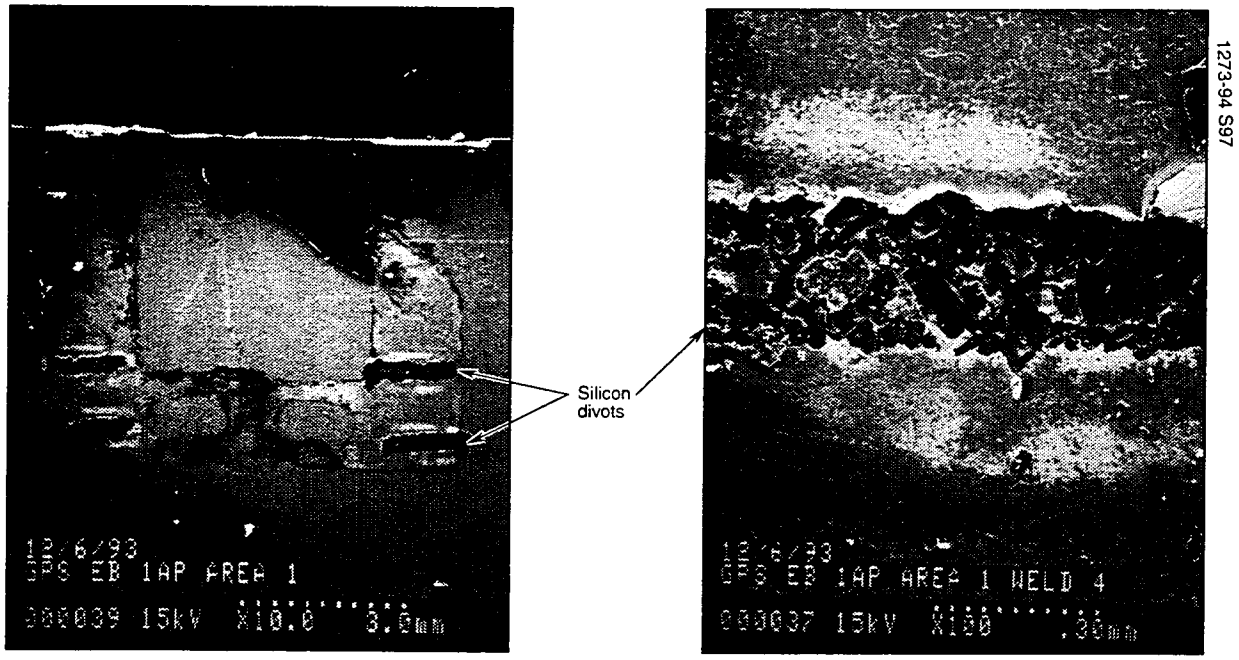

Figure 15. Photomicrographs exhibiting typical P-side fracture surfaces. (a) interblade silicon divots are present on all four welds of this tab; (b) higher magnification view exhibits sililcon structure at bottom of the divot.

original bond interface within the Si. Adjacent to the Si divots, the bright tear ridges of dimples within the Ag can easily be seen. The two broad, rectangular fracture regions adjacent to the Si divots, which correspond with the shape and location of the two electrode blades, were not as well bonded with the tab as were the center sections. The dimples in these regions are much smaller than the dimples around the well-bonded regions near the Si divots. The outline of the original interconnect position is delineated by a collection of debris on the Ag layer.

The physical layout of N- and P-side vapor-deposited layers differ slightly. Also the thermal mass and the heat-transfer characteristics of the two sides differ. Hence, weld variations will occur based on these factors alone, and simply applying the same weld parameters to both the N and the P sides will not necessarily result in comparable weld quality. The original weld parameters formed good-quality P-side welds, but the N-side welds were of a lesser quality. Original N-side welds did not exhibit evidence of a bond between the cell and interconnect in the region between the two electrode blades. The regions directly under the blades form first. During the subsequent stages of welding, the interblade regions form.

Energy dispersive X-rays (EDX) were used in the SEM to identify the chemical species on the fracture surfaces. The dimples that formed were, in every case, Ag on both the cell side and the interconnect side of the interface. The divots in the Si cell on the P-side welds were the only instances where the bond failed somewhere other than between the Ag layers on the cell and on the interconnect. No peaks attributable to the Invar core were found in the EDX analyses of the fracture surfaces.

Metallographic cross sections were made of the as-fabricated welds. Figure 16 exhibits a typical P-side weld cross section. In Figure 16b, a columnar grain structure is evident across the entire weld interface. Initial welds made on the N side of the GPS cells resulted in welds that did not exhibit grain growth across the interface. Modifications to the original GPS weld parameters improved the weld integrity and resulted in N-side weld cross sections with evidence of good metallurgical bonding. Metallographic cross sectioning is also useful for determining the amount of interface porosity, or void content. A porous interface will fail more quickly in fatigue loading than an interface with little or no porosity. Hence, porosity is undesirable. The interface exhibited in Figure 16b contains very little porosity.

Specimens tested by ASEC personnel far surpassed the minimum pull strength thought necessary to meet mission requirements. If failure occurs in the interconnect material during a pull test, then any variation in strength values is indicative of a variation in interconnect strength. For this reason, it is best to use a peel test, which better evaluates the weld strength, instead of the interconnect strength. Qualitative strength comparisons were made in MMTC during the manual peel portion of the destructive physical analysis. In general, the GPS welds offered considerable resistance both before and after thermal cycling. Often the cell was cracked by the operator before the tab peeled off. Many of the welds exhibited divots in the solar cell through to the Si layer (Figure 17). The divots were in the interblade region. Though there were many welds that failed with Si divots, there was still noticeable and sometimes significant variations in weld quality amongst the welds across one cell, as determined from the resistance offered during tab removal and by the fracture surface.

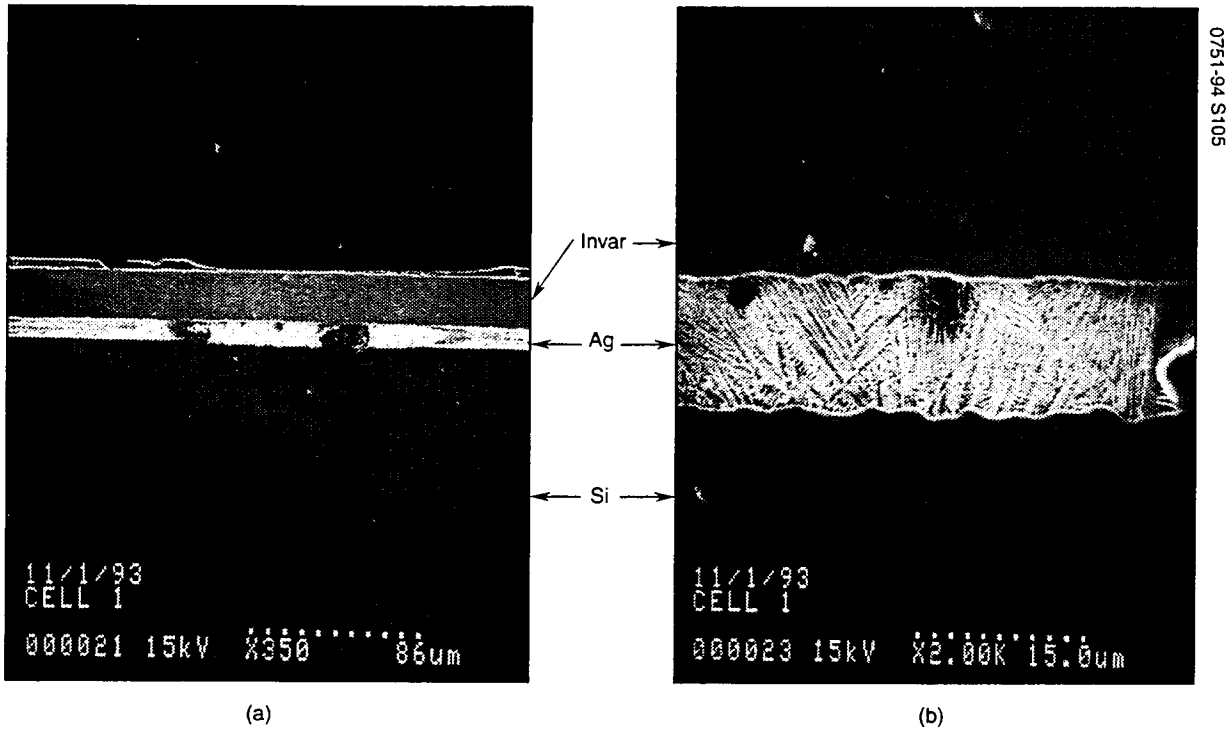

Figure 16. Photomicrographs of a metallographic cross section exhibiting weld between P-side tab and Si solar cell. Columnar grains across original interface are evident in (b).

Figure 17. Typical fracture surface of modified N-side weld with Si divot.

Evidence of melting was often found on the external surface of strongly attached tabs (Figure 18). EDX analyses confirmed the presence of Ag, Fe, and Ni on the top surface of the tab. This and the appearance of the tab surface indicate that surface melting occurred during welding, and that interdiffusion occurred between the different material layers in the tab. Concerns existed that surface melting of the interconnect was detrimental to the bond integrity. However, this was not the case. A moderate degree of surface melting was found to be favorable because it is a readily detectable indicator of heat input and a likely indicator of interface melting.

Fatigue-type fracture should initiate from the perimeter of the weld and work inwards with additional cycles. After 3720 cycles between –146 and +71°C, however, the perimeter of the "good welds" did not exhibit fatigue-type features. It was difficult to find evidence of thermal-fatigue fracture on most of the thermal-cycled welds. Fatigue fracture was evident only on the welds exhibiting the poorest appearance and the weakest peel strengths.

The post-thermal-cycle P-side welds observed in the SEM after the tabs had been removed exhibited a high percentage of failures within the Si solar cells. In these cases, the welds were so strong

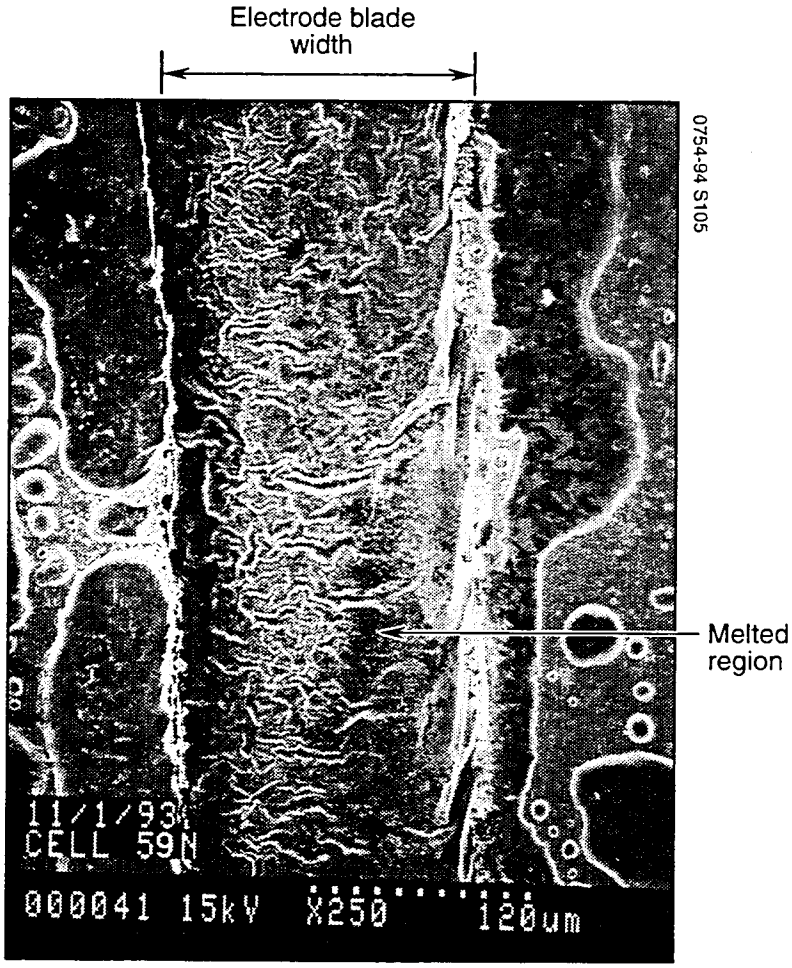

Figure 18. Photomicrograph of top of the Ag-plated tab exhibiting evidence of melting.

that the bond failed within the Si. Divots within the cell are evident at extremely low magnifications (Figure 15). Occasionally a very small P-side weld that ultimately failed by fatigue was found amongst a majority of high-strength, high-quality welds. No explanation was readily available to explain the anomalous results.

The high number of adherent welds and small amount of thermal-fatigued fracture surface may be the result of several factors. First, the weld strength may far exceed the stresses that were induced at the interface. Second, the stresses, because of the CTEs involved and the physical layout of the tabs, may be low. Third, the number of thermal cycles may have been insufficient to induce a fatigue failure for the given stress level. The samples that exhibited evidence of fatigue failure were those that appeared the smallest in size. The large physical difference between the strong and weak welds often resulted in an equally large difference in fatigue strength. In short, there was margin in the "good weld" strength—the majority of the welds on these cells would not fail in fatigue if the number of thermal cycles were to increase slightly. The welds produced for GPS appear to surpass their mission requirement. The GPS cells utilize Ag-plated Invar, which more closely matches the thermal-expansion behavior of the Si cell, hence, lowering the induced stresses. A similar material change would most likely have a similar positive effect on the survival of DMSP welds.

3.3 Mechanical Cycling

MM's weld production specification calls for use of a pull test on solar cell/interconnect test samples to monitor possible changes in the weld process on a day-to-day basis. Variations from normal pull strengths are expected to alert the operator that the weld machine is not operating properly. The pull test usually resulted in failure away from the weld, and, hence, as previously stated, tested the strength of the mesh and not the weld. Furthermore, it said little about the weld's potential fatigue strength. Static strength and fatigue strength are related but are not equivalent. The mechanical fatigue tests performed during this investigation were not intended as a direct replacement of the thermal tests. Rather, this testing was seen as a means of quickly evaluating changes in fabrication parameters. The stresses induced by mechanical fatigue cannot exactly duplicate the stresses induced by thermal fatigue. The limitations of accelerated thermal and mechanical fatigue testing must be appreciated when comparing this data with thermal fatigue data.

Many variables affect the welds' fatigue properties. The dominant variable affecting the fatigue properties is the quality of the weld. Apparently equivalent samples would be tested under equivalent conditions, yet the fatigue strength of the two samples would differ significantly (Figure 19). Upon further investigation, it was determined that the difference in original weld quality between the two samples was responsible for the disparate strengths. The amount of porosity, the weld area, and the extent of pre-existing damage all contribute to weld quality.

Much of the quality variation is inherent in the mesh design. The physical configuration of the mesh being welded may differ from one end of the cell to the other because the mesh may not be aligned perfectly parallel to the solar cell. Because of alignment variations, welds at different locations will be made at various shaped portions of the mesh structure. Welds may be made at the center of the "X" in the mesh or across the legs. This will affect the area in contact with the

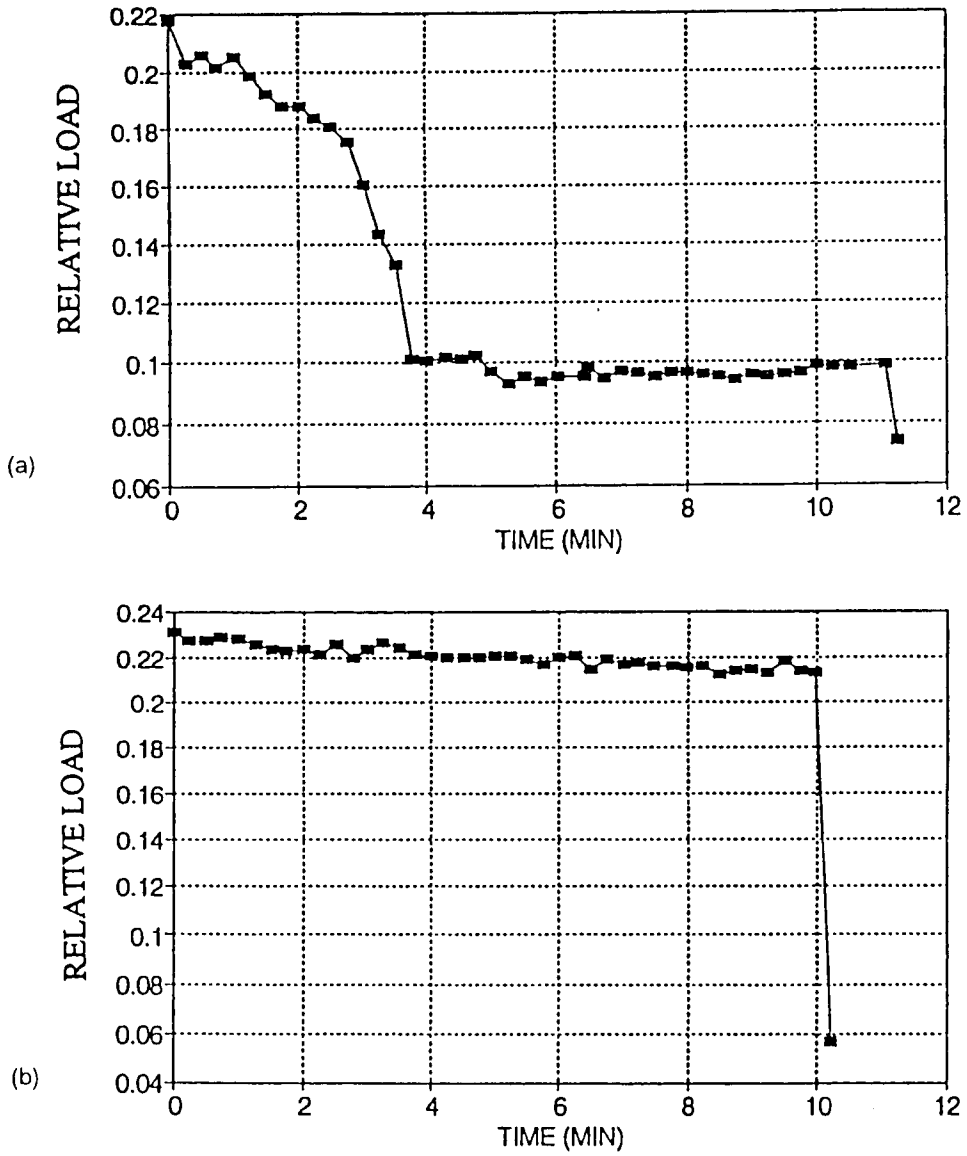

Figure 19. Fatigue strength data for two similarly loaded samples differing in weld quality. (a) Diffuse, weak welds; (b) stronger welds.

cell during welding and, consequently, the weld quality and stress state. Though the chem-etched mesh is considerably smoother than the expanded mesh, irregularities in both the cell and the mesh will also result in local weld variations.

Sample preparation also had a significant effect on the fatigue properties. Any slight imperfection along the border of the mesh tended to concentrate stress. During the testing, the mesh strand closest to this imperfection would fail first, thereby reducing the mesh cross section and further concentrating the stress in that local area. Tests such as these typically produced fatigue

plots in which the load dropped off due to the mesh strands breaking (Figure 20). Since the fatigue machine was set to run at a constant displacement, a drop in cross-sectional area resulted in a drop in the load-carrying capacity of the remaining mesh. During a "successful" test, the load dropped off progressively as the welds slowly failed (Figure 21). The similarity between these two plots demonstrates the need for post-test physical examinations of the samples to properly classify the failure mode.

No repeatable change in the fatigue properties were noticed among the samples prepared with different configurations. The mechanical fatigue tester proved unable to verify predictions that changes in the location of the welds on the mesh and slits in the mesh between each setdown would affect the mesh fatigue properties. It was felt that variations in original weld quality overshadowed any effects caused by changes in weld location or mesh slitting.

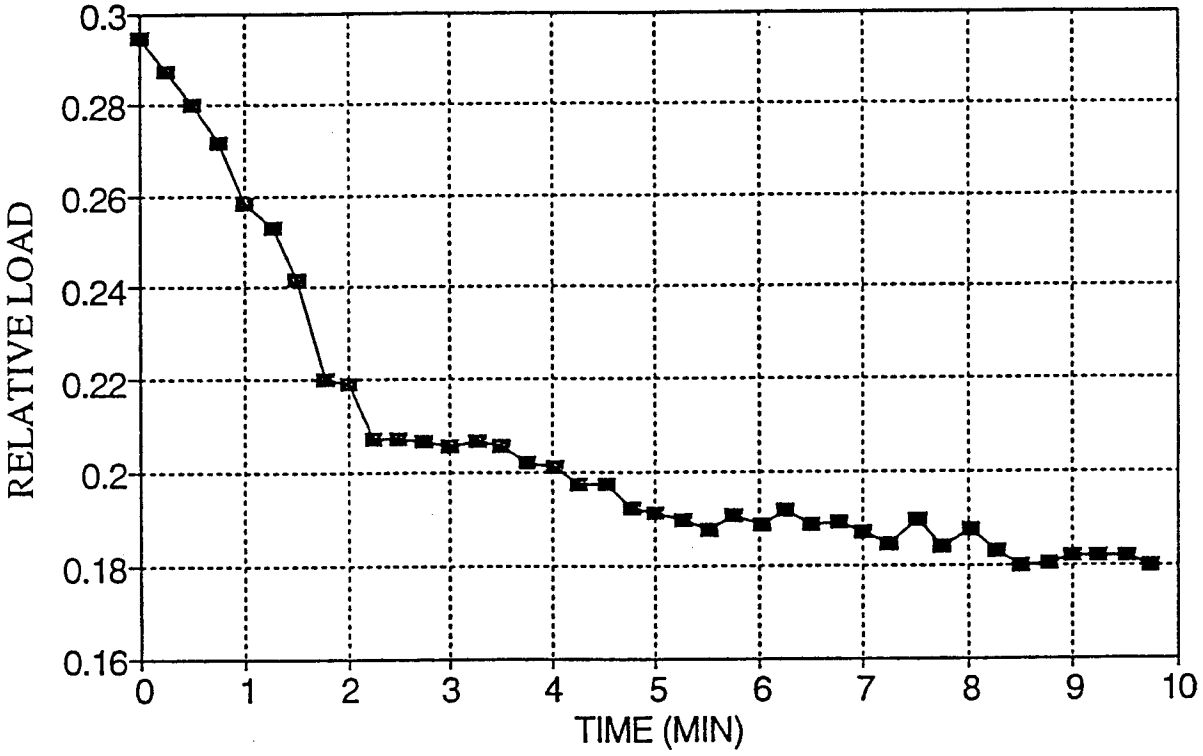

Figure 20. Fatigue strength for sample in which the mesh ripped during the test.

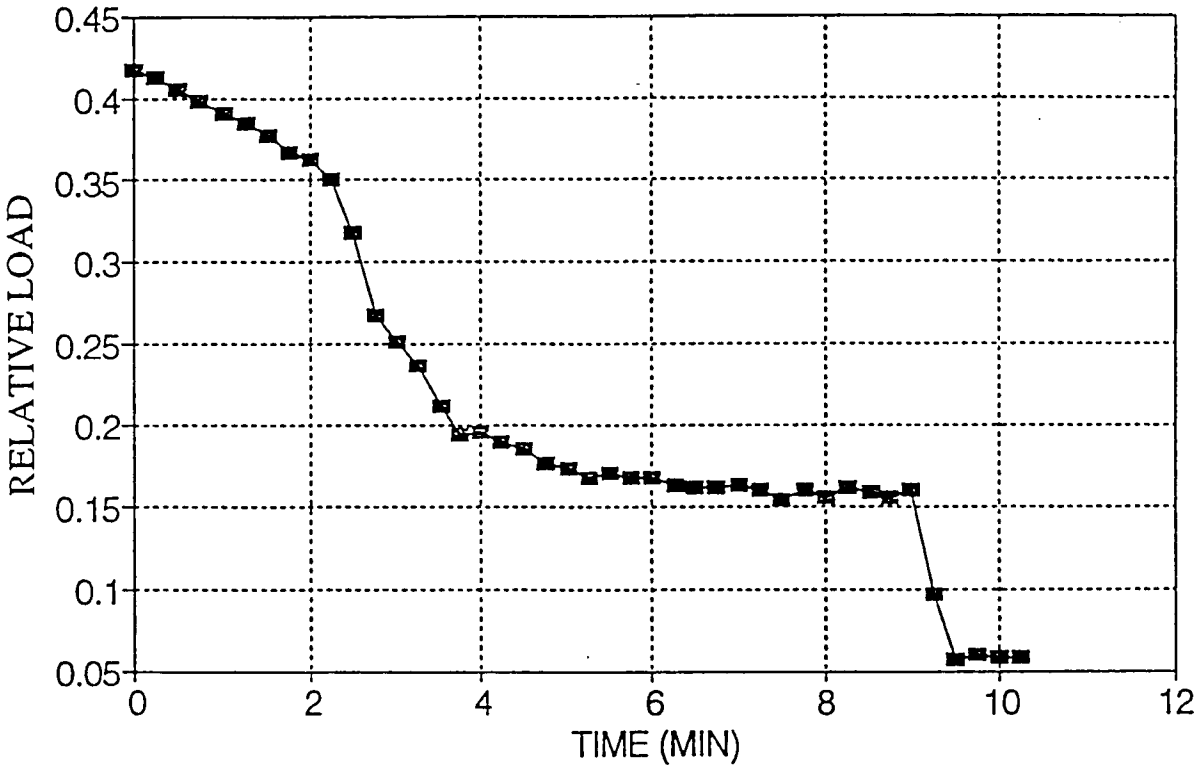

Figure 21. Fatigue strength data for sample in which the welds failed progressively without ripping the mesh.

Though the mechanical fatigue tester suffered from high weld-quality sensitivity, it was possible to use the test in a pass/fail capacity. It was possible to discern between extremely "bad" welds and very "good" welds. On the P side, a 0.5"-wide mesh connected to two setdowns and deflected approximately 0.0034" per cycle would fail if the weld quality was poor and would not fail after 15,000 cycles if the weld quality was good. Under these conditions, the mesh was cycled between approximately 0.3 and 0.9 lb.

3.4 Thermal Cycling

The thermal-cycling performance of etched-mesh Ag interconnect samples as determined from tests between LN_2 temperature and 85°C is exhibited in Figures 22 and 23. The weld failures were typically progressive, as opposed to catastrophic failure of any given multiple-weld solar cell. The N-side samples performed in a fairly consistent manner. After 1000 cycles, the typical P-side sample failed its last remaining setdown. A typical N-side sample remained adherent for slightly longer. This is in agreement with the results obtained from investigations of samples thermal cycled by MM where it was noted that the P-side welds failed before the N-side welds.

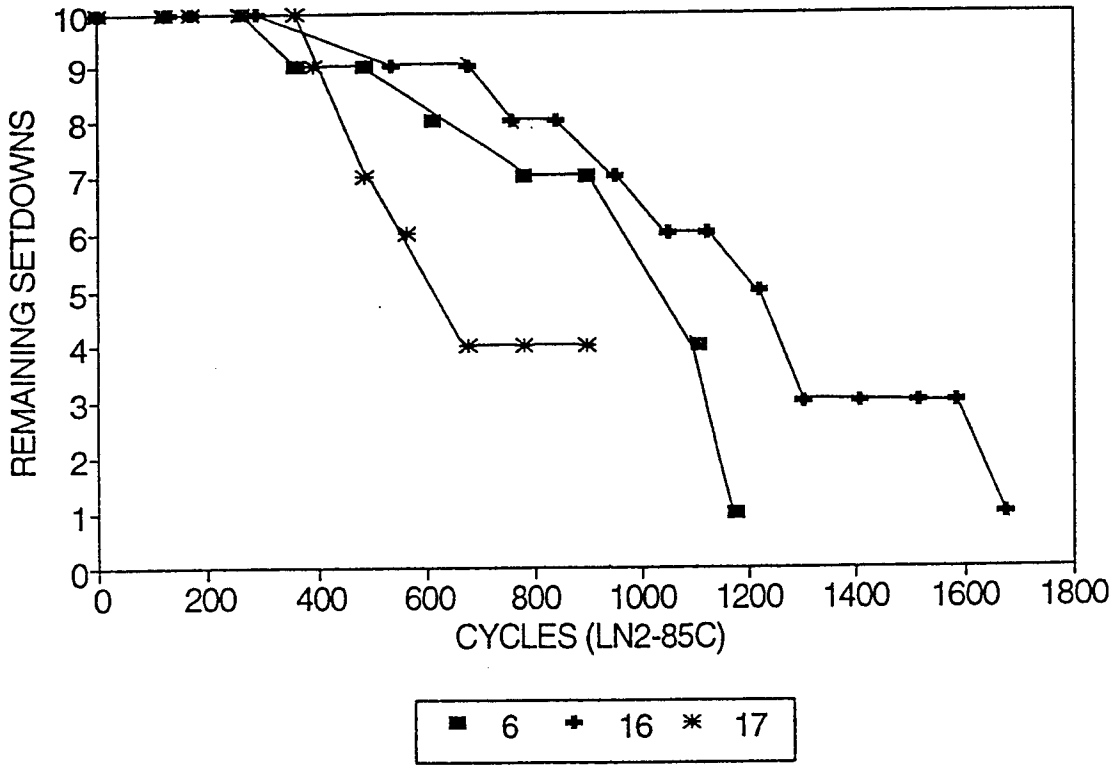

Figure 22. Experimental data exhibiting trends in survivability behavior of etched mesh N-side welds. Lines delineate general trends only. All N-side welds are nominal configuration.

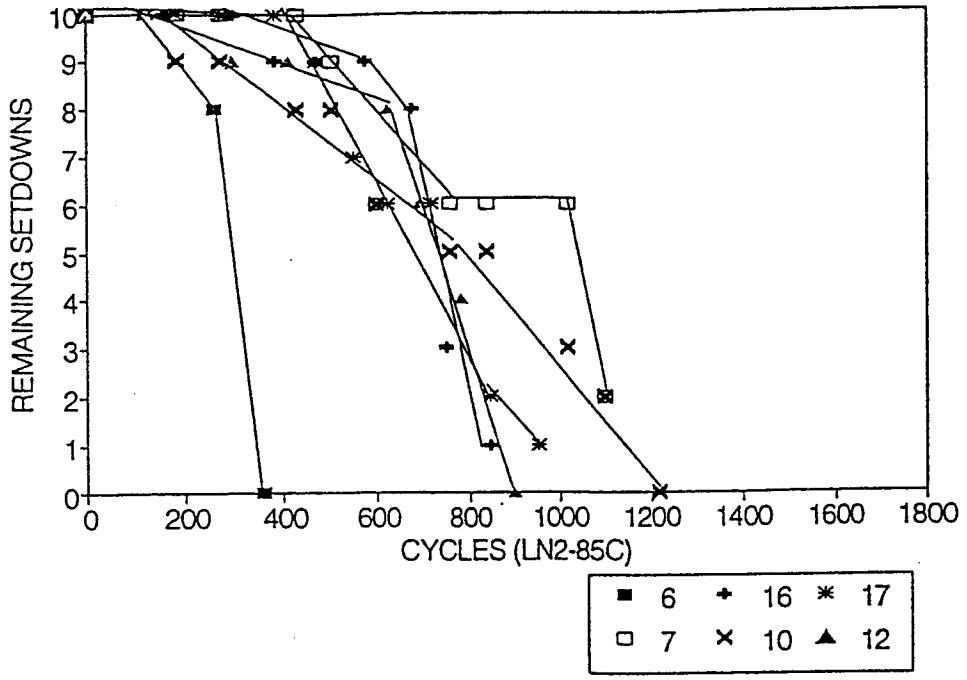

Figure 23. Experimental data exhibiting trends in survivability behavior of etched mesh P-side welds. Different mesh configurations are represented. Lines delineate general trends only. Slit samples: 6, 10, 16, 17; nominal samples: 7, 12; mesh on edge of cells.

Etched mesh samples performed much better than expanded mesh samples. The weld size for the same size electrode setdown was much bigger, of higher quality, and more consistent on the etched mesh samples than on the expanded mesh samples. The absence of residual stresses from the mesh-forming operation, present for the expanded mesh, also helped the etched mesh survive longer. Much of the variation in expanded mesh cyclic performance is a result of the inherently large variation in weld quality typical of expanded mesh samples.

Sample-to-sample variations were still a problem with the etched mesh samples. The performance of samples was a direct function of the weld quality on those samples. Weld quality was typically consistent across any given cell. Individual welds of high quality were seldom found adjacent to setdowns with poor-quality welds. A distribution of failure rates was statistically expected.

Numerical modeling of the solar array by the Structural Technology Department suggests that different mesh configurations would have an effect on the weld survival rates. Samples of various configurations were prepared and tested. Slits, according to the modeling, act to separate the individual setdowns and prevent them from having an effect on each other. P-side welds placed on the edge of the cell were designed to be physically similar to the N-side welds, which, according to empirical findings, survived better than the P-side welds. Additional cells welded in the nominal fashion were cut along the edge of the mesh to place the existing welds close to the edge of the mesh but still in the center of the cell. Schematics of the different sample configurations are given in Figure 5. According to the modeling, the slit samples should perform better than the unslit samples since each setdown can act individually and is not subject to the stresses and strains felt by the other setdowns. The number of test specimens affects the validity of the results. Because of inherent scatter, a high number of samples should be tested to reveal possible trends. If the weld quality is exceptionally good, performance trends will be revealed with fewer samples.

During the course of this testing, in agreement with observations from earlier thermal cycling tests, the setdowns on the edge failed first. Mesh separation characteristically progressed inward from the two sides of the cell. This was typically observed throughout the course of this investigation. Variations due to non-uniform weld quality occasionally upset this trend. The slits and welds on the edge of the cell did not degrade the weld performance. However, as in the case of the mechanical fatigue testing, the effects of intentional changes in mesh geometry were overshadowed by the quality of the individual welds. With weld quality frozen at a given level, it was best to try to minimize the stress and strain on the individual setdowns. Unfortunately, variations in weld quality still prevented the models, which proposed stress and strain reduction techniques, from being verified in a conclusive and cost-effective manner. The testing was successful, however, in confirming the number of cycles to failure that was predicted by the modeling for this temperature range. The testing was also successful in confirming the difference in survivability between N- and P-side welds. On average, the P-side welds failed prior to the N-side welds. Observations of original weld size on uncycled N- and P-side welds did not reveal massive differences between the two sides. However, there was a large difference between the two sides in the remaining weld area adherent to the cell after thermal cycling. This may be the result of different stress levels acting on the two sides because of physical configurations, different thermal behavior, or better-quality welds within the same weld area.

4. Conclusions

1. Solar-cell interconnect fatigue behavior correlated strongly with initial weld quality. Efforts to reduce interconnect stresses in a Ag mesh of constant thickness were of secondary importance to efforts to improve weld quality. Wide variations in weld quality masked changes in fatigue behavior resulting from changes in other parameters. Complete validation of theoretical stress models and stress-reducing mesh geometries, hence, could not be provided through mechanical or thermal fatigue tests without testing a prohibitively large number of samples necessary for statistically valid comparisons. Mesh modifications designed to reduce the stress acting on individual welds (other than mesh thickness) were not detrimental to the weld survivability; however, the program schedule, weld quality variations, and limited sample size prevented a proper evaluation. A reduction in mesh thickness substantially improved weld survival rates.

2. The choice of interconnect material was critical to weld quality. Chem-etched Ag mesh samples produced a more uniform weld compared to expanded Ag mesh samples; however, the inherent high thermal conductivity and low electrical resistance of an all-Ag interconnect inhibited development of a strong metallurgical bond between the cell and mesh. Ag-plated Invar, by contrast, has a much lower thermal conductivity, and it was possible to produce a much hotter weld in a localized region and promote good metallurgical bonding.

3. The choice of interconnect material and design was also critical to the effective stress state. The close CTE match between Si and Invar resulted in lower stresses being generated in the GPS cells during thermal cycling. The large CTE difference and resultant high stress generated in an all-Ag interconnect prompted most solar-array manufacturers to long ago abandon the all-Ag design.

4. A mechanical fatigue tester designed for this investigation can be used to evaluate welds in a pass/fail capacity. The tester provides a quick-look capability for pass/fail decisions, but is inadequate to evaluate slight changes in parameters. The fatigue tester reliably cycled small resistance welds through deflections as small as 0.003". These deflections translate into loads less than 1 lb.

5. The fatigue performance of a cell with a few high-quality welds can often surpass the performance of a cell with multiple lesser-quality welds.

6. Thermal cycling tests were able to confirm a discrepancy in the average cycles to failure between N- and P-side Ag mesh welds, as predicted by theoretical modeling. The number of cycles to failure, as determined from the testing, was close to the number of cycles predicted by the modeling. These results, while not conclusive, indicate that the Aerospace theoretical stress models were "in the ballpark," and the stress-reducing mesh modifications predicted from the models were of merit.

proper metallurgical bond. A material change and interconnect design change would be necessary to produce an interconnect assembly capable of meeting mission requirements.

8. The GPS interconnect surpasses the mission requirements. A better choice of material, as compared to DMSP, lower stresses and fewer thermal cycles combine to produce a high-quality solar cell interconnect. The interconnect material choice allowed for development of strong metallurgical bonds and excellent thermal cycling performance.

References

1. P. C. Brennan, J. A. Wasynczuk, "Weld Integrity Evaluation of Interconnections for Solar Cells," ATM (3476-05)-3, April 29, 1993.

2. P. C. Brennan, "Weld Integrity Evaluation of DMSP Solar Cell Interconnections," ATM (3478-20)-7, July 23, 1993.

3. P. C. Brennan, "Mechanical Fatigue Testing of DMSP Solar Cell Welded Interconnections," ATM 93(3478-20)-10, September 23, 1993.

4. P. C. Brennan, R. A. Brose, "Weld Evaluation of ASEC-Produced GPS Solar Cells," ATM (4470-03)-2, November 2, 1993.

5. P. C. Brennan, R. A. Brose, "Evaluation of Thermal-Cycled ASEC-Produced GPS Solar Cells," ATM (4470-03)-3, December 14, 1993.

6. P. C. Brennan, "Thermal Cycle Testing of DMSP Solar Cell Welded Interconnects," ATM 94(4478-20)-6, April 27, 1994.

7. Comsat Technical Review, Comsat Laboratories, Vol. 4, No 1, 53-78, 1974.

TECHNOLOGY OPERATIONS

The Aerospace Corporation functions as an "architect-engineer" for national security programs, specializing in advanced military space systems. The Corporation's Technology Operations supports the effective and timely development and operation of national security systems through scientific research and the application of advanced technology. Vital to the success of the Corporation is the technical staff's wide-ranging expertise and its ability to stay abreast of new technological developments and program support issues associated with rapidly evolving space systems. Contributing capabilities are provided by these individual Technology Centers:

Electronics Technology Center: Microelectronics, solid-state device physics, VLSI reliability, compound semiconductors, radiation hardening, data storage technologies, infrared detector devices and testing; electro-optics, quantum electronics, solid-state lasers, optical propagation and communications; cw and pulsed chemical laser development, optical resonators, beam control, atmospheric propagation, and laser effects and countermeasures; atomic frequency standards, applied laser spectroscopy, laser chemistry, laser optoelectronics, phase conjugation and coherent imaging, solar cell physics, battery electrochemistry, battery testing and evaluation.

Mechanics and Materials Technology Center: Evaluation and characterization of new materials: metals, alloys, ceramics, polymers and their composites, and new forms of carbon; development and analysis of thin films and deposition techniques; nondestructive evaluation, component failure analysis and reliability; fracture mechanics and stress corrosion; development and evaluation of hardened components; analysis and evaluation of materials at cryogenic and elevated temperatures; launch vehicle and reentry fluid mechanics, heat transfer and flight dynamics; chemical and electric propulsion; spacecraft structural mechanics, spacecraft survivability and vulnerability assessment; contamination, thermal and structural control; high temperature thermomechanics, gas kinetics and radiation; lubrication and surface phenomena.

Space and Environment Technology Center: Magnetospheric, auroral and cosmic ray physics, wave-particle interactions, magnetospheric plasma waves; atmospheric and ionospheric physics, density and composition of the upper atmosphere, remote sensing using atmospheric radiation; solar physics, infrared astronomy, infrared signature analysis; effects of solar activity, magnetic storms and nuclear explosions on the earth's atmosphere, ionosphere and magnetosphere; effects of electromagnetic and particulate radiations on space systems; space instrumentation; propellant chemistry, chemical dynamics, environmental chemistry, trace detection; atmospheric chemical reactions, atmospheric optics, light scattering, state-specific chemical reactions and radiative signatures of missile plumes, and sensor out-of-field-of-view rejection.

THE AEROSPACE CORPORATION
2350 E. El Segundo Boulevard
El Segundo, California 90245-4691
U.S.A.